Criterion for Distinguishing Sequential from Nonsequential Contributions to the Double Ionization of Helium in Ultrashort Extreme-Ultraviolet Pulses

Aihua Liu* and Uwe Thumm†
James R. Macdonald Laboratory, Department of Physics, Kansas State University, Manhattan, Kansas 66506, USA
(Received 1 May 2015; published 28 October 2015)

We quantify sequential and nonsequential contributions in two-photon double ionization of helium atoms by intense ultrashort extreme-ultraviolet pulses with central photon energies $\hbar\omega_{\mathrm{ctr}}$ near the sequential double-ionization threshold. If the spectrum of such pulses overlaps both the sequential ($\hbar\omega > 54.4$ eV) and nonsequential ($\hbar\omega < 54.4$ eV) double-ionization regimes, the sequential and nonsequential double-ionization mechanisms are difficult to distinguish. By tracking the double-ionization asymmetry in joint photoelectron angular distributions, we introduce the two-electron forward-backward-emission asymmetry as a measure that allows the distinction of sequential and nonsequential contributions. Specifically, for $\hbar\omega_{\mathrm{ctr}} = 50$ eV pulses with a sine-squared temporal profile, we find that the sequential double-ionization contribution is the largest at a pulse length of 650 as, due to competing temporal and spectral constraints. In addition, we validate a simple heuristic expression for the sequential double-ionization contribution in comparison with *ab initio* calculations.

DOI: 10.1103/PhysRevLett.115.183002 PACS numbers: 32.80.Rm, 33.80.Rv, 42.50.Hz

In 1975, the mechanism of nonsequential double ionization was revealed in the photoionization of alkaline earth atoms [1]. It is enabled by strong electronic correlation and thus clearly distinct from the sequential double-ionization mechanism. Nonsequential double ionization was observed for noble gas atoms in 1982 [2] and received rapidly increasing attention from both experimentalists [3–9] and theorists [10–13].

Photoelectron angular distributions of single-photon double ionization were found to owe their structure partly to (dipole) selection rules [11,14,15] and to consist of symmetrical and antisymmetrical contributions (with regard to electron exchange), that each can be written as the product of an angular and a correlation factor [11]. For coplanar emission geometry, where the emitted-electron momenta and polarization axis of the linearly polarized extreme-ultraviolet (XUV) pulse lie in a plane, and for equal energy sharing (equal asymptotic kinetic energies E_1 and E_2 of the photoelectrons), the angular factor becomes $|\cos\theta_1 + \cos\theta_2|^2$, where θ_1 and θ_2 are photoelectron emission angles relative to the polarization direction of the ionizing light, while the electron correlation factor follows as $\exp\{-4\ln 2[(\theta_{12}-\pi)/\theta_{1/2}]^2\}$, with the mutual emission angle $\theta_{12} = |\theta_1 - \theta_2|$. The adjustable parameter, $\theta_{1/2}$, is related to the significance of correlation in the double-ionization process [11]. The antisymmetrical contribution and back-to-back electron emission vanish at equal energy sharing but become progressively more prominent for increasingly nonequal energy sharing, as the antisymmetrical contribution $|\cos\theta_1 - \cos\theta_2|^2$ gradually appears in joint photoelectron angular distributions [10,11,16].

Figure 1(a) shows our *ab initio*-calculated joint angular distributions $P(\theta_1, \theta_2; \varepsilon)$ for single-photon double ionization, the central XUV-pulse photon energy $\hbar\omega_{\mathrm{ctr}} = 90$ eV, and coplanar emission geometry. Our joint angular distributions [17] agree well with experimental results [9] and show that symmetrical electron emission

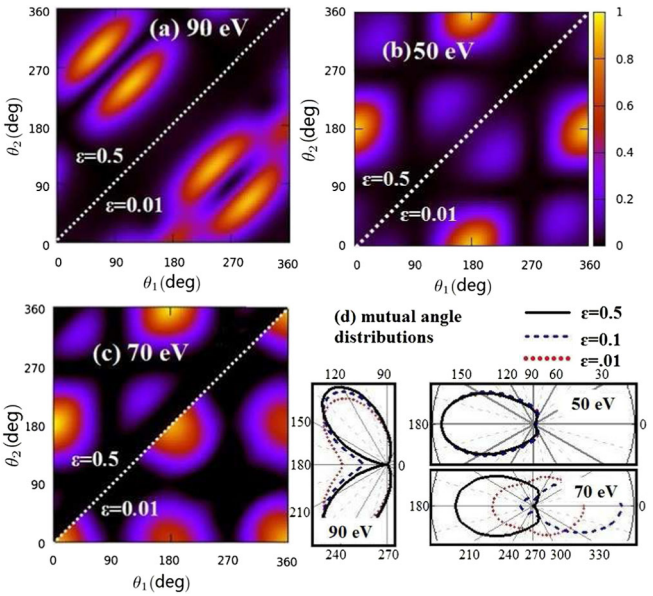

FIG. 1 (color online). Calculated joint angular distributions for the single- and two-photon double ionization of helium in an (a) $\hbar\omega_{\mathrm{ctr}} = 90$, (b) 50, and (c) 70 eV sine-squared XUV pulse with peak intensities of 10^{14} W/cm^2 and total pulse lengths of 1 fs (364 as full width at half maximum in intensity). (a) Single- and (b),(c) two-photon double ionization. Upper left panels: Equal energy sharing. Bottom right panels: Extremely unequal energy sharing. (d) Corresponding mutual angular distributions for energy sharings $\varepsilon = 0.01, 0.1$, and 0.5.

remains dominant over a wide interval of energy-sharing parameters $\varepsilon = E_1/(E_1 + E_2)$. This weak dependence on ε is also seen in the mutual angular distributions for $\hbar\omega_{\mathrm{ctr}} = 90$ eV in Fig. 1(d), which display double-ionization yields as a function of θ_{12} and are normalized individually to the total (angle-integrated) yield [16].

For sufficiently long XUV pulses, two-photon double ionization of helium atoms proceeds sequentially if the central XUV photon energy $\hbar\omega_{\mathrm{ctr}}$ is larger than the second ionization potential ($I_2 = 54.4$ eV) and nonsequentially for $(I_1 + I_2)/2 = 39.5$ eV $< \hbar\omega_{\mathrm{ctr}} < I_2$, where $I_1 = 24.6$ eV is the first ionization potential of helium. For such pulses, sequential double ionization and nonsequential double ionization are clearly distinguishable. Two-photon double ionization is much more difficult to detect than single-photon double ionization due to its extremely small total cross section ($\approx 10^{-52}$ cm^4 s) [17–19]. It was first measured in 2005 [18], followed by many theoretical studies [16,17,19–25].

If the spectral profile of an ultrashort XUV pulse overlaps the sequential and nonsequential double-ionization regimes, the distinction between sequential double ionization and nonsequential double ionization becomes difficult. Furthermore, for extremely short pulse durations of less than a few hundred attoseconds, strong electronic correlation is enforced, even for central pulse energies in the sequential regime [24]. In this case, the time between the two photoabsorption events is so short that the interelectronic distance remains sufficiently small to entail strong correlation of the released electrons. Accordingly, calculated joint angular distributions for double ionization at $\hbar\omega_{\mathrm{ctr}} = 70$ eV dramatically change for decreasing XUV pulse length, moving from a product of two independent dipole distributions in the long-pulse limit (a few femtoseconds) to progressively forward-backward asymmetrical distributions with increasingly suppressed emission of both electrons in the same direction along the XUV polarization direction (forward emission), resembling joint angular distributions for nonsequential double ionization.

The role of electronic correlation in two-photon double ionization of helium with ultrashort XUV pulses was investigated in previous *ab initio* calculations [24], yet it remains unclear how to *quantitatively* characterize and distinguish sequential and nonsequential contributions. In this Letter, we investigate joint angular distributions for the double ionization of helium and refer to the degree of two-electron forward-backward-emission asymmetry (i.e., the normalized difference between both electrons being emitted in the same hemisphere and in opposite hemispheres centered about the laser-polarization direction) as a measure for the relative importance of sequential double ionization. We calculate joint angular distributions by numerically solving *ab initio* the time-dependent Schrödinger equation (TDSE), expanding the atomic wave function in the four angular variables of the two electrons. Based on convergence tests [17], we include orbital and total angular quantum numbers up to 3 in this expansion. We employ the finite-element (FE) discrete-variable representation (DVR) scheme and propagate the two-electron radial wave functions on a numerical grid for the electrons' radial coordinates r_1 and r_2. We partition the numerical grid into 100–200 FEs (adjusting the number of FEs to the pulse duration) and use four DVR basis functions in each FE. A detailed description of our implementation of this method is given in Ref. [17]. Unless stated otherwise, we use atomic units. Throughout this work, we assume XUV pulses with sine-squared temporal profiles and peak intensities of 10^{14} W/cm^2 and discuss angular distributions for coplanar emission geometry.

Absorption of two photons by singlet ground-state helium atoms produces interfering S and D partial waves, which one might expect to result in more structured joint angular distributions than for single-photon double ionization. However, as pointed out by Kheifets and Ivanov [21], two-photon double-ionization angular distributions consist of five terms that include electronic correlation effects as similar Gaussian factors and can be divided into symmetrical and antisymmetrical components, in analogy to the single-photon double-ionization angular distributions discussed above. Figure 1 shows our calculated joint [Figs. 1(b) and 1(c)] and mutual [Fig. 1(d)] angular distributions for two-photon double ionization by XUV pulses with a pulse length of 1 fs and central photon energies of 50 [Figs. 1(b) and 1(d)] and 70 eV [Figs. 1(c) and 1(d)], separately normalized to their respective angle-integrated yields. While the angular distributions for the photon energy $\hbar\omega_{\mathrm{ctr}} = 50$ eV in the nonsequential double-ionization regime are virtually indistinguishable for different energy sharings [23], for $\hbar\omega_{\mathrm{ctr}} = 70$ eV, i.e., in the sequential double-ionization regime, the character of the angular distribution changes from being strongly dominated by back-to-back emission at equal energy sharing ($\varepsilon = 0.5$) to dominant forward (side-by-side) emission at extremely unequal energy sharing ($\varepsilon = 0.01$).

The equal-energy-sharing joint angular distributions for $\hbar\omega_{\mathrm{ctr}} = 50$ [Fig. 1(b)] and 70 eV [Fig. 1(c)] are similar and dominated by back-to-back emission, with two weak peaks along the $\theta_2 = 360° - \theta_1$ diagonal, indicating symmetrical emission, with no side-by-side ($\theta_2 = \theta_1$) emission. At unequal energy sharing and for $\hbar\omega_{\mathrm{ctr}} = 70$ eV [bottom right panel in Fig. 1(c)], back-to-back emission ($\theta_{12} = 180°$) remains strong, but side-by-side emission becomes dominant, since the importance of electronic repulsion in double ionization decreases with decreasing energy sharing ε. The photoelectrons thus become more efficiently sequentially released in the same direction by the XUV electric field, leading to strong side-by-side emission and, specifically, to the forward-dominated mutual angular distributions for $\varepsilon = 0.1$ and 0.01 in Fig. 1(d).

For the *total* pulse length τ (given by the separation of successive nodes of the sine-squared temporal pulse

profile) of 1 fs and a corresponding spectral width of 6 eV (full width at half maximum in intensity), the spectra of the 50 and 70 eV XUV pulses considered above are confined to the nonsequential or sequential double-ionization regime, respectively. For significantly shorter pulse lengths, the distinction between these two double-ionization spectral regimes becomes less obvious.

In order to investigate the effect of spectral pulse overlap with the two double-ionization regimes, we show in Fig. 2 conditional two-photon double-ionization angular distributions for a fixed emission angle of one electron ($\theta_1 = 0°$) and $\hbar\omega_{\mathrm{ctr}} = 50$ eV XUV pulses with total pulse durations of 160 as, 500 as, and 3 fs, corresponding to spectral pulse widths (full width at half maximum in intensity) of 37, 12, and 2 eV, respectively. They show dominant back-to-back emission and minor peaks for emission into the same ("forward") hemisphere. The normalized back-to-back emission yields for the two shown energy-sharing values and three pulse lengths are almost identical. The small forward-emission yields are displayed separately in the enlarged right panels. In contrast to the large back-to-back-emission yields, the forward-emission yields depend on the energy sharing and pulse length. They increase as the energy sharing changes from equal ($\varepsilon = 0.5$) to extremely unequal ($\varepsilon = 0.01$). This increase is most pronounced at the intermediate pulse length of 500 as [Fig. 2(b)]. The relatively strong forward emission for $\varepsilon = 0.01$ is reminiscent of the forward-emission dominance in sequential double ionization [cf. Fig. 1(c)]. Reducing the pulse length from 3 fs to 500 as thus lends sequential double-ionization character to the angular distribution. This trend is reversed by further reducing the pulse length from 500 to 160 as, since the constraint for double ionization to happen during the presence of the ultrashort 160 as pulse reinforces electronic correlation, suppressing sequential emission.

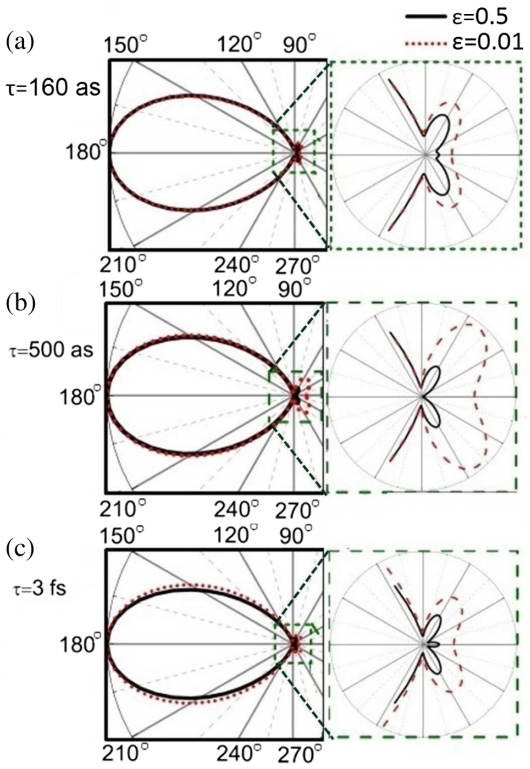

FIG. 2 (color online). Conditional angular distributions with one electron emitted along the XUV linear polarization direction ($\theta_1 = 0°$) for two-photon double ionization of helium in XUV pulses with a central photon energy of 50 eV and total pulse lengths of (a) 160 as, (b) 500 as, and (c) 3 fs. Each graph shows results for equal ($\varepsilon = 0.5$) and extremely unequal ($\varepsilon = 0.01$) energy sharing. The full-range distributions (left panels) are normalized to their maxima. The right panels enlarge the forward-emission contributions.

The preceding discussion suggests the sequential double-ionization contribution to have a lower pulse-length limit given by a temporal constraint while being limited at larger pulse durations by vanishing spectral overlap with the sequential double-ionization spectral domain. In order to quantitatively distinguish sequential double ionization from nonsequential double-ionization contributions, we evaluate the two-electron forward-backward asymmetry parameter

$$A(\theta_1 = 0;\varepsilon) = \frac{(\int_{-\pi/2}^{\pi/2} - \int_{\pi/2}^{3\pi/2})P(0,\theta_2;\varepsilon)d\theta_2}{(\int_{-\pi/2}^{\pi/2} + \int_{\pi/2}^{3\pi/2})P(0,\theta_2;\varepsilon)d\theta_2} \quad (1)$$

for the XUV-pulse durations, energy-sharing parameters, and central XUV-pulse energy considered in Fig. 2, including, in addition, calculations for $\varepsilon = 0.1$ and 0.3. The limiting cases of both electrons being emitted into the same hemisphere and into opposite hemispheres correspond to asymmetries of 1 and -1, respectively. As shown in Fig. 3, the asymmetry for 160 as and 3 fs pulse durations are large in magnitude ($A \approx -0.99$) and comparatively insensitive to changes in energy sharing. In contrast, the asymmetry for 500 as pulses more strongly depends on the energy sharing.

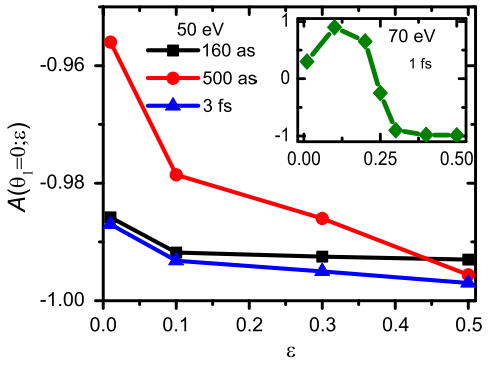

FIG. 3 (color online). Two-electron forward-backward-emission asymmetries $A(\theta_1 = 0;\varepsilon)$ of the conditional angular distributions in Fig. 2 and, additionally, for $\varepsilon = 0.1$ and 0.3. The inset shows asymmetries for XUV pulses with a central photon energy of 70 eV and 1 fs total pulse length, corresponding to the angular distributions in Fig. 1(c). Markers represent *ab initio* calculations and are straight-line interpolated.

It falls in between the asymmetries for 160 as and 3 fs pulses at equal energy sharing and increases to −0.956 at extremely unequal energy sharing ($\varepsilon = 0.01$). This weak energy-sharing dependence of $A(\theta_1;\varepsilon)$ for pulses centered in the nonsequential double-ionization regime is in sharp contrast with asymmetry changes from ≈ 1 to ≈ -1 for XUV pulses with $\hbar\omega_{\mathrm{ctr}} = 70$ eV in the sequential double-ionization regime and 1 fs total pulse duration, shown in the inset in Fig. 3 [cf. Fig. 1(c)].

The inset in Fig. 4 shows the spectral intensity $I(\omega)$ of a $\tau = 1$ fs sine-squared XUV pulse with $\hbar\omega_{\mathrm{ctr}} = 50$ eV. A small portion of $I(\omega)$ overlaps the sequential double-ionization regime. Since $I(\omega)$ decreases rapidly above the second ionization threshold, the XUV-pulse spectral components in the sequential double-ionization regime primarily account for double ionization with small excess kinetic energies of the emitted electrons, $E_1 + E_2 = 2\hbar\omega - 79.0$ eV, and extremely unequal energy sharing. For example, a typical frequency component of the pulse in the sequential double-ionization regime at $\hbar\omega = 54.8$ eV results in the highly unequal energy sharing with $\varepsilon = (\hbar\omega - 54.4\ \mathrm{eV})/(2\hbar\omega - 79.0\ \mathrm{eV}) = 0.013$. We therefore choose a small value, $\varepsilon = 0.01$, for the following discussion. The stars in Fig. 4 show the asymmetries $A(\theta_1 = 0;\varepsilon = 0.01)$ derived from our *ab initio* FE-DVR numerical solution of the TDSE according to Eq. (1) for total XUV-pulse lengths between 160 as and 2.5 fs. Consistent with Figs. 2 and 3, the asymmetries are largest near 500 as.

Attempting to find a simple analytical description of the pulse-length dependence of A in Fig. 4, we first recall the known expression for the sequential double-ionization yield [22,26],

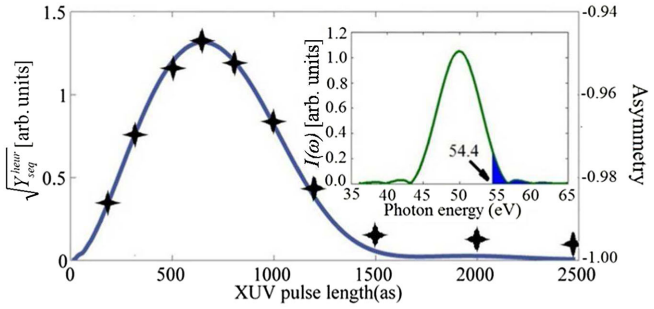

FIG. 4 (color online). Comparison of *ab initio*-calculated two-electron forward-backward double-ionization asymmetries $A(\theta_1 = 0;\varepsilon = 0.01)$ (stars) with the square root of the heuristic expression [Eq. (3)] for the sequential double-ionization contribution $Y^{\mathrm{heur}}_{\mathrm{seq}}$ (solid blue line) as a function of the total XUV-pulse length for a central pulse energy of 50 eV. $\sqrt{Y^{\mathrm{heur}}_{\mathrm{seq}}}$ is normalized to the maximum of A at 650 as. The inset shows the spectral intensity of a $\hbar\omega_{\mathrm{ctr}} = 50$ eV pulse with sine-squared temporal profile and a total pulse length of 1 fs. The blue area indicates the overlap of the pulse spectrum with the spectral domain for sequential double ionization at $\hbar\omega > 54.4$ eV.

$$Y_{\mathrm{seq}} = \frac{\sigma_1\sigma_2 I_0^2}{\omega^2}(T_{\mathrm{eff}})^2, \tag{2}$$

given in terms of the single-photon single-ionization cross sections for He (σ_1) and He^+ (σ_2) and the effective interaction time of the XUV pulse for the single-photon processes, T_{eff}. For sine-squared pulses, T_{eff} equals 3/8 times the total XUV-pulse duration [19,23,26].

Guided by the sequential double-ionization yield of Eq. (2), we integrate over the sequential double-ionization frequency range to construct the heuristic expression

$$Y^{\mathrm{heur}}_{\mathrm{seq}} = B\left[T_{\mathrm{eff}}\int_{I_2}^{\infty}\frac{I(\omega)}{\omega}d\omega\right]^2 \tag{3}$$

for the sequential double-ionization contribution, uniting the constraints on sequential double ionization given by (i) the temporal pulse profile (factor T^2_{eff}) and (ii) spectral overlap with the sequential double-ionization spectral domain (factor $[\int_{I_2}^{\infty}\frac{I(\omega)}{\omega}d\omega]^2$). Figure 4 shows $\sqrt{Y^{\mathrm{heur}}_{\mathrm{seq}}}$ (blue solid line) for $\hbar\omega_{\mathrm{ctr}} = 50$ eV after normalizing the proportionality constant B to our *ab initio* results (stars). The normalized heuristic sequential double-ionization contribution reaches its maximum at a pulse length of 650 as, in agreement with our *ab initio* calculation. This confirms that the sequential double-ionization yield can be neglected for pulse durations larger than 1.5 fs, as one would expect in view of the vanishing overlap between the pulse spectrum and the sequential double-ionization spectral range. It also confirms the requirement of a sufficiently long pulse duration for sequential double ionization to occur, as discussed above. Accordingly, due to relatively small sequential double-ionization contributions, the asymmetries for $\tau = 160$ as and 3 fs in Fig. 3 are comparatively robust against changes in energy sharing [cf. Figs. 1(b) and 1(c)].

Based on the proportionality of $\sqrt{Y^{\mathrm{heur}}_{\mathrm{seq}}}$ and our *ab initio*-calculated forward-backward double-ionization asymmetries A, we conclude that $A + 1$ is a good indicator for the sequential double-ionization contribution to the double ionization of helium for central pulse energies in the nonsequential double-ionization spectral domain. This offers the possibility of determining the pulse lengths of ultrashort XUV pulses based on measured asymmetries A.

In summary, we studied sequential and nonsequential contributions to the two-photon double ionization of helium. We calculated photoelectron angular distributions by applying the FE-DVR numerical method to solve *ab initio* the time-dependent Schrödinger equation for helium exposed to ultrashort XUV pulses. We found that two-electron forward-backward asymmetries of two-photoelectron angular distributions constitute an appropriate measure for the distinction between sequential and nonsequential double-ionization contributions. We confirmed this link between the forward-backward asymmetry

and the sequential double-ionization contribution for central pulse energies below I_2 by matching the pulse-length-dependent profile of *ab initio*-calculated forward-backward asymmetries with an intuitively appealing heuristic formula for the square root of the sequential double-ionization fraction.

This work was supported by the U.S. National Science Foundation under Grant No. PHY-1068752 and the Division of Chemical Sciences, Office of Basic Energy Sciences, Office of Energy Research, U.S. Department of Energy.

*iwaa@phys.ksu.edu
†thumm@phys.ksu.edu

[1] V. V. Suran and I. P. Zapesnochnii, Sov. Phys–Tech. Phys. Lett. **1**, 420 (1975).
[2] A. l'Huillier, L. A. Lompre, G. Mainfray, and C. Manus, Phys. Rev. Lett. **48**, 1814 (1982); Phys. Rev. A **27**, 2503 (1983).
[3] Th. Weber, M. Weckenbrock, A. Staudte, L. Spielberger, O. Jagutzki, V. Mergel, F. Afaneh, G. Urbasch, M. Vollmer, H. Giessen, and R. Dörner, Phys. Rev. Lett. **84**, 443 (2000).
[4] B. Feuerstein R. Moshammer, D. Fischer, A. Dorn, C. D. Schröter, J. Deipenwisch, J. R. Crespo Lopez-Urrutia, C. Höhr, P. Neumayer, J. Ullrich, H. Rottke, C. Trump, M. Wittmann, G. Korn, and W. Sandner, Phys. Rev. Lett. **87**, 043003 (2001).
[5] A. Rudenko, K. Zrost, B. Feuerstein, V. L. B. de Jesus, C. D. Schröter, R. Moshammer, and J. Ullrich, Phys. Rev. Lett. **93**, 253001 (2004).
[6] B. Walker, B. Sheehy, L. F. DiMauro, P. Agostini, K. J. Schafer, and K. C. Kulander, Phys. Rev. Lett. **73**, 1227 (1994).
[7] O. Schwarzkopf, B. Krässig, J. Elmiger, and V. Schmidt, Phys. Rev. Lett. **70**, 3008 (1993).
[8] O. Schwarzkopf and V. Schmidt, J. Phys. B **29**, 1877 (1996).
[9] H. Bräuning R. Dörner, C. L. Cocke, M. H. Prior, B. Krässig, A. S. Kheifets, I. Bray, A. Bräuning-Demian, K. Carnes, S. Dreuil, V. Mergel, P. Richard, J. Ullrich, and H. Schmidt-Böcking, J. Phys. B **31**, 5149 (1998).
[10] A. S. Kheifets and I. Bray, J. Phys. B **31**, L447 (1998).
[11] A. Huetz, P. Selles, D. Waymel, and J. Mazeau, J. Phys. B **24**, 1917 (1991); L. Avaldi and A. Huetz, J. Phys. B **38**, S861 (2005).
[12] C. W. McCurdy, M. Baertschy, and T. N. Rescigno, J. Phys. B **37**, R137 (2004).
[13] A. Palacios, T. N. Rescigno, and C. W. McCurdy, Phys. Rev. A **77**, 032716 (2008).
[14] F. Maulbetsch and J. S. Briggs, J. Phys. B **26**, 1679 (1993).
[15] F. Maulbetsch and J. S. Briggs, J. Phys. B **27**, 4095 (1994).
[16] A. Liu and U. Thumm, Phys. Rev. A **91**, 043416 (2015).
[17] A. Liu and U. Thumm, Phys. Rev. A **89**, 063423 (2014).
[18] H. Hasegawa, E. J. Takahashi, Y. Nabekawa, K. L. Ishikawa, and K. Midorikawa, Phys. Rev. A **71**, 023407 (2005).
[19] X. Guan, K. Bartschat, and B. I. Schneider, Phys. Rev. A **77**, 043421 (2008).
[20] A. Palacios, T. N. Rescigno, and C. W. McCurdy, Phys. Rev. A **79**, 033402 (2009).
[21] A. S. Kheifets and I. A. Ivanov, J. Phys. B **39**, 1731 (2006).
[22] R. Pazourek, S. Nagele, and J. Burgdörfer, J. Phys. B **48**, 061002 (2015).
[23] Z. Zhang, L.-Y. Peng, M.-H. Xu, A. F. Starace, T. Morishita, and Q. Gong, Phys. Rev. A **84**, 043409 (2011).
[24] J. Feist, S. Nagele, R. Pazourek, E. Persson, B. I. Schneider, L. A. Collins, and J. Burgdörfer, Phys. Rev. Lett. **103**, 063002 (2009).
[25] S. X. Hu, Phys. Rev. Lett. **111**, 123003 (2013).
[26] J. Feist, S. Nagele, R. Pazourek, E. Persson, B. I. Schneider, L. A. Collins, and J. Burgdörfer, Phys. Rev. A **77**, 043420 (2008).